Supplementary material

S1. Numeric results of the steady-state SRAO reactors

Table S1 showed the influent/effluent result of steady-state SRAO reactors, with the end product and conversion parameters. There are totally 12 available studies to make this table, with 6 of them under heterotrophic conditions (in orange) and 6 of them under autotrophic conditions (in blue), based on which the figures in Table 1 can be made, also the conversion parameters can be obtained for analysing the stoichiometry and reaction rate of SRAO. The data in green was calculated in this study.

Table S1. The steady-state experimental results from long-term SRAO reactors. The cell in green stands for data calculated in this study.

	Influent, mg-N/L, mg-S/L, mg-COD/L				Effluent, mg-N/L, mg-S/L, mg-COD/L								Conversion		
Reference	NH_4^+	SO_4^{2-}	**COD**	N/S (mol/mol)	NH_4^+	NO_3^-	NO_2^-	N_2	SO_4^{2-}	S^0	S^{2-}	COD	❒N/❒S (mol/mol)	❒COD/❒S (mg/mgS)	TN removal rate(kg-N/m3/d)
(Fdz-Polanco, 2001)	2300	1000	27000	**5.26**	1025	N.A.	N.A.	1275	5	795	200	1950	**2.9**	**8.4**	**0.15**
(Wang et al., 2017)	1163	1200	9000	**2.22**	400	100	50	613	216	290	100	2520	**1.8**	**2.2**	**0.9**
(Zhao et al., 2006)	450	100	1750	**10.28**	193.5	N.A.	N.A.	**225**	19	71	10	525	**7.2**	**5.0**	**0.02**
(Sabumon, 2008)	350	950	3750	**0.81**	133	N.A.	N.A.	**217**	147	N.A.	N.A.	1618	**0.6**	**0.9**	**0.11**
(Zhu et al., 2022)	97	90	400	**2.47**	19	12	8	**57**	50	N.A.	N.A.	50	**4.5**	**2.9**	**0.04**
(Rikmann et al., 2016)	225	200	N.A.	**2.6**	150	N.A.	N.A.	N.A.	130	N.A.	N.A.		**2.45**	N.A.	**0.08**
(Liu et al., 2008)	210	256	N.A.	**1.9**	42	21	0	**147**	57.6	N.A.	N.A.		**1.94**	N.A.	**0.67**
(Madani et al., 2021)	138	154	N.A.	**2.1**	40	**25**	**10**	**63**	75	N.A.	N.A.		**2.8**	N.A.	**0.1**
(Zhang et al., 2009)	106	198	N.A.	**1.9**	50	<1	<1	**56**	179	N.A.	<1		**0.59**	N.A.	0.04
(Qin et al., 2021)	70	80	N.A.	**2.0**	39	5	2	**24**	72	N.A.	2		8.9	N.A.	0.05
(Yang et al., 2009)	50	73	N.A.	**2.3**	30	N.A.	N.A.	**16**	48	**7**	N.A.		**1.83**	N.A.	0.01

S2. Steady-state conversion efficiency of ammonium and sulfate

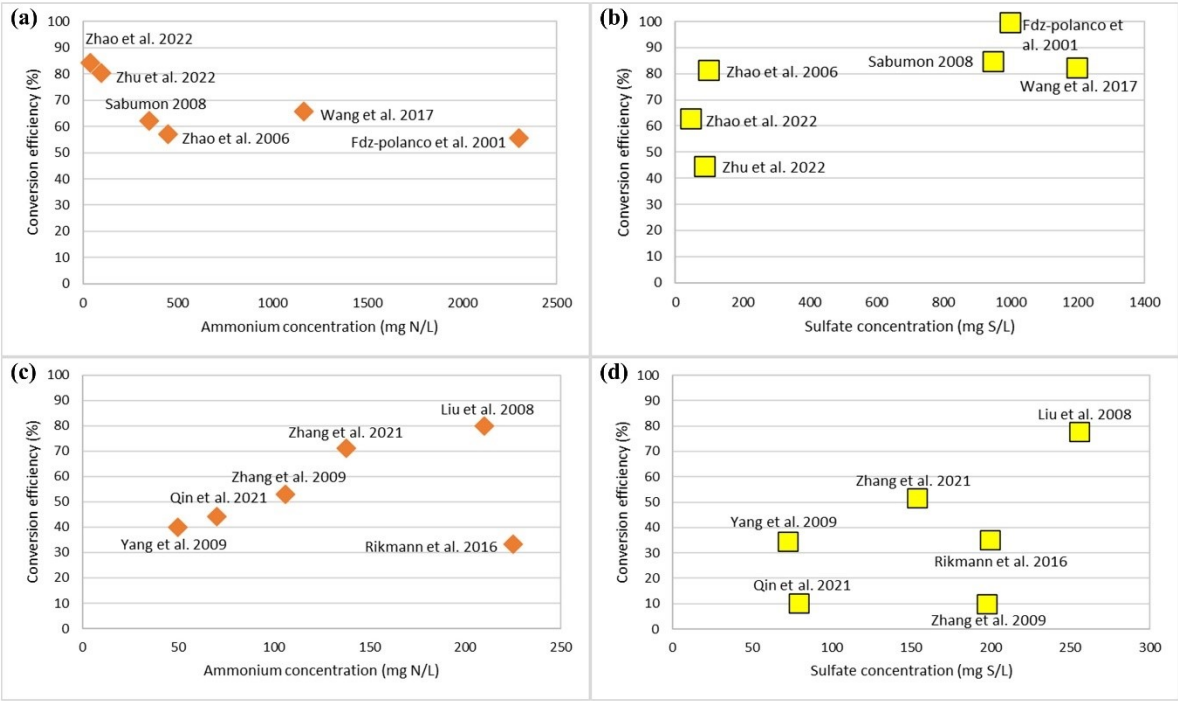

Fig. S1. Effect of influent substrate concentration on the conversion efficiency of ammonium (left) and sulfate (right), under heterotrophic conditions (top) and autotrophic condition (bottom) in different studies

To investigate the effect of influent concentration on the removal capacity under heterotrophic condition, Fig. S1 (a)(b) illustrates the relation between influent substrate concentration and the corresponding conversion efficiency. In the analysed literatures (the environmental conditions were similar), the ammonium conversion efficiencies were found close to each other, which seemed irrelevant to the influent ammonium concentration. As for the conversion amount of sulfate, few conclusions can be drawn due to the coexistence of heterotrophic sulfate reduction.

Regarding to autotrophic conditions as shown in Fig. S1(c)(d), it is observed that as the influent ammonium concentration increases, the conversion efficiency exhibits an increase, which differs from the case under organic carbon conditions. The reason might be the enrichment of functional biomass, as autotrophic biomass is more likely to be enriched in

high-concentration conditions. Conversely, no distinct pattern is observed for sulfate conversion.

S3. Calculation process of the overall pathways

Table S2. Detailed calculations for complex autotrophic SRAO reaction 1A (see Figure 1 and Table 3)

Factor	Substrate/product☎ Microbial process	NH_4^+	NO_3^-	NO_2^-	N_2	S^{2-}	S^0	SO_4^{2-}	H^+	H_2O	Organic-e^-	ΔG_0(kJ/mol/eq)	ΔG_0(kJ/mol/e-)
						SRAO-N_2-S^0 reaction, pathway 1: Elementary reaction							
1x	Sulfammox-N_2-S^0 (1A)	**-2**			**1**		**1**	**-1**		**4**		-47.8	-8.0
						pathway 2: SRAO -NO_3^--S^{2-} + SAD (NO_3^-; S_2^-) + SAD (NO_2^-; S^0)							
2x	Sulfammox-NO_3-S^{2-} (1D)	**-1**	**1**			**1**		**-1**	**2**	**1**		309.9	38.7
+													
2x	SD (NO_3^-; S_2^-) (2A)		**-1**	**1**		**-1**	**1**		**-2**	**1**		2.2	1.1
+													
1x	SD (NO_2^-; S^0) (2D)			**-2**	**1**		**-1**	**1**				-670.2	-111.7
						pathway 3: SRAO -NO_3^--S^0 + SAD (NO_3^-; S^0) + SAD (NO_2^-; S^0)							
2/3x	Sulfammox-NO_3-S^0 (1C)	**-3**	**3**				**4**	**-4**	**-2**	**7**		1302.1	54.3
+													
2/3x	SAD (NO_3^-; S^0) (2B)		**-3**	**3**			**-1**	**1**	**2**	**-1**		-211.6	-35.3
+													
1x	SAD (NO_2^-; S^0) (2D)			**-2**	**1**		**-1**	**1**				-670.2	-111.7
						pathway 4: SRAO -NO_2^--S^0 + SAD (NO_2^-; S^0)							
2x	Sulfammox-NO_2-S^0 (1E)	**-1**		**1**			**1**	**-1**		**2**		312.4	52.1
+													
1x	SAD (NO_2^-; S^0) (2D)			**-2**	**1**		**-1**	**1**				-670.2	-111.7
						pathway 5: SRAO -NO_2^--S^0 + nitrite anammox							
1x	Sulfammox-NO_2-S^0 (1E)	**-1**		**1**			**1**	**-1**		**2**		312.4	52.1
+													
1x	Anammox (4)	**-1**		**-1**	**1**					**2**		-357.5	-119.2
						pathway 6: SRAO -NO_3^--S^{2-} + SAD (NO_3^-; S^0) + SAD (NO_2^-; S^0)							

1x	Sulfammox-NO_3-S^{2-} (1D)	**-1**	**1**			**1**		**-1**	**2**	**1**		309.9	38.7
+													
1x	SAD (NO_3^-; S_2^-) (2A)		**-1**	**1**		**-1**	**1**		**-2**	**1**		2.2	1.1
+													
1x	Anammox (4)	**-1**		**-1**	**1**					**2**		-357.5	-119.2
pathway 7: SRAO -NO_3^--S^0 + SAD (NO_3^-; S^0) + nitrite anammox													
1/3x	Sulfammox-NO_3-S^0 (1C)	**-3**	**3**				**4**	**-4**	**-2**	**7**		1302.1	54.3
+													
1/3x	SAD (NO_3^-; S^0) (2B)		**-3**	**3**			**-1**	**1**	**2**	**-1**		-364.9	-60.8
+													
1x	Anammox (4)	**-1**		**-1**	**1**					**2**		-357.5	-119.2

Factor	Substrate/product☎ Microbial process	NH_4^+	NO_3^-	NO_2^-	N_2	S^{2-}	S^0	SO_4^{2-}	H^+	H_2O	Organic-e^-	ΔG_0(kJ/mol/eq)	ΔG_0(kJ/mol/e-)
SRAO -N_2-S^{2-} reaction, pathway 1: Elementary reaction													
1x	Sulfammox-N_2-S^{2-} (1B)	**-8**			**4**	**3**		**-3**	**8**	**12**		-551.9	-23.0
SRAO -N_2-S^{2-} reaction, pathway 2: Sulfammox-NO_2^--S^{2-} + Nitrite anammox													
1x	Sulfammox-NO_2^--S^{2-} (1F)	**-4**		**4**		**3**		**-3**	**8**	**4**		878.2	36.6
+													
4x	Anammox (4)	**-1**		**-1**	**1**					**2**		-357.5	-119.2

Table S3. Calculation process of 1B

Factor	Substrate/product ☎ Microbial process	NH_4^+	NO_3^-	NO_2^-	N_2	S^{2-}	S^0	SO_4^{2-}	H^+	H_2O	Organic-e$^-$	CO_2	ΔG_0(kJ/mol/eq)	ΔG_0(kJ/mol/e-)
SRAO with organic carbon, pathway 1: SRAO -NO_3^--S^{2-} + Hetero-denitrification (NO_3^-) + Hetero-denitrification (NO_2^-)														
2X	**SRAO** -NO_3-S^{2-} (1D)	**-1**	**1**			**1**		**-1**	**2**	**1**			309.9	38.7
+														
1X	Hetero-denitrification (NO_3^-) (3A)		**-2**	**2**						**4/3(methanol); 1(acetate); 1(glucose)**	**-2/3(methanol); -1/2(acetate); -1/6(glucose)**	**2/3(methanol); 1(acetate); 1/6(glucose)**	-314.1(methanol); -298.7(acetate); -330.8(glucose)	-78.5(methanol); -74.7(acetate); -82.7(glucose)
+														
1X	Hetero-denitrification (NO_2^-) (3B)			**-2**	**1**				**-2**	**3(methanol); 5/2(acetate); 5/2(glucose)**	**-1(methanol); -6/8(acetate); -6/24(glucose)**	**1(methanol); 12/8(acetate); 36/24(glucose)**	-776.4(methanol); -753.4(acetate); -801.6(glucose)	-129.4(methanol); -125.6(acetate); -133.6(glucose)
=	Hetero- **SRAO** -1	**-2**			**1**	**2**		**-2**	**2**	**19/3(methanol); 11/2(acetate); 11/2(glucose)**	**5/3(methanol); 20/8(acetate); 10/4(glucose)**	**-5/3(methanol); 10/8(acetate); 5/12(glucose)**	-470.7(methanol); -432.3(acetate); -512.6(glucose)	-47.1(methanol); -43.2(acetate); -51.3(glucose)
SRAO with organic carbon, pathway 2: SRAO -NO_2^--S^{2-} + Hetero-denitrification (NO_2^-)														
2X	**SRAO** -NO_2^--S^{2-} (1F)	**-4**		**4**		**3**		**-3**	**8**	**4**			878.2	36.6
+														
1X	Hetero-denitrification (NO_2^-) (3B)			**-2**	**1**				**-2**	**3(methanol); 5/2(acetate); 5/2(glucose)**	**-1(methanol); -6/8(acetate); -6/24(glucose)**	**1(methanol); 12/8(acetate); 36/24(glucose)**	-776.4(methanol); -753.4(acetate); -801.6(glucose)	-129.4(methanol); -125.6(acetate); -133.6(glucose)
=	Hetero- **SRAO** 2	**-4**			**2**	**3**		**-3**	**4**	**10(methanol); 9(acetate); 9(glucose)**	**2(methanol); 3(acetate); 3(glucose)**	**-2(methanol); 6/4(acetate); 1/2(glucose)**	-674.6(methanol); -628.6(acetate); -725.0(glucose)	-52.2 (methanol); -52.4(acetate); -60.4(glucose)
SRAO with organic carbon, pathway 3: SRAO -NO_3^--S^0 + Hetero-denitrification (NO_3^-) + Hetero-denitrification (NO_2^-)														
2X	**SRAO** -NO_3-S^0 (1C)	**-3**	**3**				**4**	**-4**	**-2**	**7**			1302.1	54.3
+														
3X	Hetero-denitrification (NO_3^-) (3A)	Hetero-denitrification (NO_3^-) (3A)		**-2**	**2**						**4/3(methanol);1(acetate);1(glucose)**	**-2/3(methanol); -1/2(acetate); -1/6(glucose)**	2/3(methanol); 1(acetate); 1/6(glucose)	-314.1(methanol); -298.7(acetate); -330.8(glucose)
+														
3X	Hetero-denitrification (NO_2^-) (3B)	Hetero-denitrification (NO_2^-) (3B)			**-2**	**1**				**-2**	**3(methanol);5/2(acetate);5/2(glucose)**	**-1(methanol); -6/8(acetate); -6/24(glucose)**	1(methanol); 12/8(acetate); 36/24(glucose)	-776.4(methanol); -753.4(acetate); -801.6(glucose)
=	Hetero- **SRAO** 3	**-6**			**3**		**8**	**-8**	**-10**	**27(methanol); 49/2(acetate); 49/2(glucose)**	**5(methanol); 60/8(acetate); 30/4(glucose)**	**-5(methanol); 30/8(acetate); 5/4(glucose)**	-667.3(methanol); -552.1(acetate); -793.0(glucose)	-22.0(methanol); -18.0(acetate); -26.4(glucose)
SRAO with organic carbon, pathway 4: SRAO -NO_2^--S^0 + Hetero-denitrification (NO_2^-)														
2X	**SRAO** -NO_2-S^0 (1E)	**-1**		**1**			**1**	**-1**		**2**			312.4	52.1
+														
1X	Hetero-denitrification (NO_2^-) (3B)	Hetero-denitrification (NO_2^-) (3B)			**-2**	**1**				**-2**	**3(methanol);5/2(acetate);5/2(glucose)**	**-1(methanol); -6/8(acetate); -6/24(glucose)**	1(methanol); 12/8(acetate); 36/24(glucose)	-776.4(methanol); -753.4(acetate); -801.6(glucose)
=	Hetero- **SRAO** 4	**-2**			**1**		**2**	**-2**	**-2**	**7(methanol); 13/2(acetate); 13/2(glucose)**	**1(methanol); 12/8(acetate); 6/4(glucose)**	**-1(methanol); 6/8(acetate); 1/4(glucose)**	-151.6(methanol); -128.6(acetate); -176.8(glucose)	-25.2(methanol); -21.4(acetate); -29.5(glucose)

Table S4. Calculation process of the complex heterotrophic SRAO pathways, for various organic carbon sources (methanol, acetate, glucose)

S4. Operation conditions of the SRAO reactors in the literature

Reactor specifications and **initial intention**	Acclimation time (days)	Seed sludge	Reference
Heterotrophic			
EGSB, 1.96L, HRT=21h. **Anaerobic digestion**	52	Anaerobic fermentation sludge	(Wang et al. 2017)
Anaerobic fluidized bed reactor, 1.5L. **Anaerobic digestion**	40	Anaerobic tank sludge from yeast factory	(Fdz-polanco. et al. 2001)
Up-flow hybrid reactor, 1.75L, HRT=2d **Sulfammox with organic carbon**	60	Activated sludge from tannery sewage, VSS/TSS=0.58	(Sabumon 2008)
Anaerobic attached-growth reactor, 3.8L **Sulfammox with organic carbon**	156	Anaerobic sludge from sulfate-rich sewage plant	(Zhao et al. 2006)
Sequencing batch reactor, 250mL, cycle time=48h. **Sulfammox with organic carbon**	90	Anammox mixed with anaerobic tank sludge, TSS=2.2 g/L	(Zhu et al. 2022a)
Autotrophic			
Non-woven rotating biological contactor, 1.7L, HRT=6h. **Anammox**	45	Anammox sludge, VSS=0.32 g/L	(Liu et al. 2008)
Sequencing batch reactor, 1.5L, cycle time=108.25h. **Sulfammox with inorganic carbon**	60	Anaerobic digestion sludge from municipal sewage plant, VSS=15 g/L	(Zhang et al. 2009)
Self-designed mixed reactor, 5L, HRT=1B. **Sulfammox with inorganic carbon**	61	Activated sludge from municipal sewage plant, VSS=3.5 g/L	(Zhang et al., 2019)
UASB, 0.75L, HRT=1B. **Sulfammox with inorganic carbon**	50	Anaerobic sludge from yeast factory	(Rikmann et al., 2014)
UASB, 3.93L, HRT=1.5d. **Sulfammox with inorganic carbon**	60	Nitrifying sludge from municipal plant, VSS=1.56 g/L	(Yang et al. 2009)
UASB, 10L, HRT=16h. **Sulfammox with inorganic carbon**	158	Anammox sludge, VSS=1.4 g/L	(Qin et al. 2021)
Up-flow anaerobic reactor, 1.7L, HRT=12-24h. **Sulfammox in mature leachate treatment**	23	Anammox sludge, VSS=1.78 g/L	(Zhan et al. 2023)

Table S5. Reactor operation conditions of the literature

S5. Gibbs free energy calculation

The standard Gibbs free energy of formation (ΔG_0) has been widely used for checking the thermodynamical feasibility of a given chemical reaction. The defined condition was set as 298.15 K (25°C), 1 atm. The involved substances in this study were listed in Table S6.

Table S6. Standard Gibbs free energy of formation under standard conditions (Rudolf K. Thauer 1977)

Substrate	NH_4^+	NO_3^-	NO_2^-	N_2	S^{2-}	S^0	SO_4^{2-}	H^+	H_2O	Methanol	Glucose	Acetate	CO_2
Standard $-\Delta G_0$ (kJ/mol)	79.4	111.3	37.2	0	85.8	0	744.6	0	237.2	175.4	915.4	369.4	394.4

$$\Delta G_0 = \left[\sum Y_{product} \Delta G_{0_{product}}\right] - \left[\sum Y_{substrate} \Delta G_{0_{substrate}}\right]$$

Where Y presents for stoichiometric coefficient of substrate and product; $\Delta G_{0product}$ and $\Delta G_{0substrate}$ can be found in Table S6. If $\Delta G_0 < 0$, then the equation can be marked as thermodynamically feasible.

However, the standard Gibbs free energy of formation considers H^+ has an activity of 1 mol/kg, which is in equivalence to pH=0. For biochemical reactions, the proton concentration should be corrected to a proper value of physiological conditions, which is normally taken by pH=7. the corrected standard Gibbs free energy of formation ΔG_0^* can be calculated by the following equation (Kleerebezem and Van Loosdrecht, 2010).

$$\Delta G_0^* = \Delta G_0 + R \cdot T \cdot m_H \cdot \ln [H^+]$$

Where ΔG_0 is the standard Gibbs free energy of formation; R is gas constant, 8.314 J/mol/K; T is thermodynamic temperature, K; $[H^+]$ is the concentration of proton, here it is 10^{-7} mol/kg. By correcting the standard Gibbs free energy of formation, the thermodynamical feasibility of microbial reactions can be better checked.

In addition to the standard Gibbs free energy of formation, it is worth noting that the actual Gibbs free energy is more dynamic, driven by the concentration difference between the substrates and products, as shown in the following equation.

Given a reaction equation, aA + bB ✂ cC + dD, the Gibbs free energy is calculated by

$$\Delta G = \Delta G_0 + R \cdot T \cdot \ln \frac{[C]^c[D]^d}{[A]^a[B]^b}$$

Where [A][B] and [C][D] are the concentrations of the substrates and products, respectively. It literally means that by introducing more substrates into the system to broaden the gap between the concentrations of substrates and products, the thermodynamical feasibility of the reaction can be improved.

The actual Gibbs free energy was able to be checked by making the assumption that the concentration of substrates, i.e., $[NH_4^+]$ and $[SO_4^{2-}]$ equals to 100 mM, the concentration of the substrates are 5 times greater than the product. The actual Gibbs free energy can be derived as a function of nitrate/nitrite byproduct rate. As a result, the thermodynamics of the SRAO reactions can be double checked via standard Gibbs free energy and actual Gibbs free energy.

As shown in Fig. S2, with the increase of nitrate/nitrite byproduct proportion (f), the ❒G and ❒G_0 value increases accordingly. At some point, it will turn from negative to positive, which means it will become thermodynamically unfavourable. The turning point varies among the

reactions. For SRAO reactions with elemental sulfur as end products (Fig. S2a and S2c), it only allows 5-9% of nitrate, or 8-12% of nitrite existed as byproduct, whereas for SRAO reactions with sulfide as end products (Fig. S2b and S2d), 18-36% of nitrate or 24-51% of nitrite can be produced as byproducts. This result is consistent with the observation of nitrite and nitrate in the previous experiments, but it is not able to pick out which reactions are taking place in reality out of the infinite possibilities.

Overall, SRAO reactions with sulfide as end products tend to be more thermodynamically favourable than that with elemental sulfur as end products, which indicates that from a thermodynamic perspective elemental sulfur might not be the main product of SRAO reactions, as usually stated in previous studies. The ❒G and ❒G_0 of SRAO reactions with sulfide as end products can reach -20 to -40 KJ/electron, while the SRAO reactions with elemental sulfur as end products can barely approach a negative Gibbs free energy change.

Due to the low efficiency of SRAO reactions, the substrate concentrations were usually 2-5 times of the products concentrations (Table S1), making the actual ❒G always more negative than ❒G_0 (Fig.1). Therefore, in reality the thermodynamic potential of SRAO reactions can be considered stronger than the standard value ❒G_0. All those SRAO reactions that have ❒G_0<0 are thereby thermodynamic feasible.

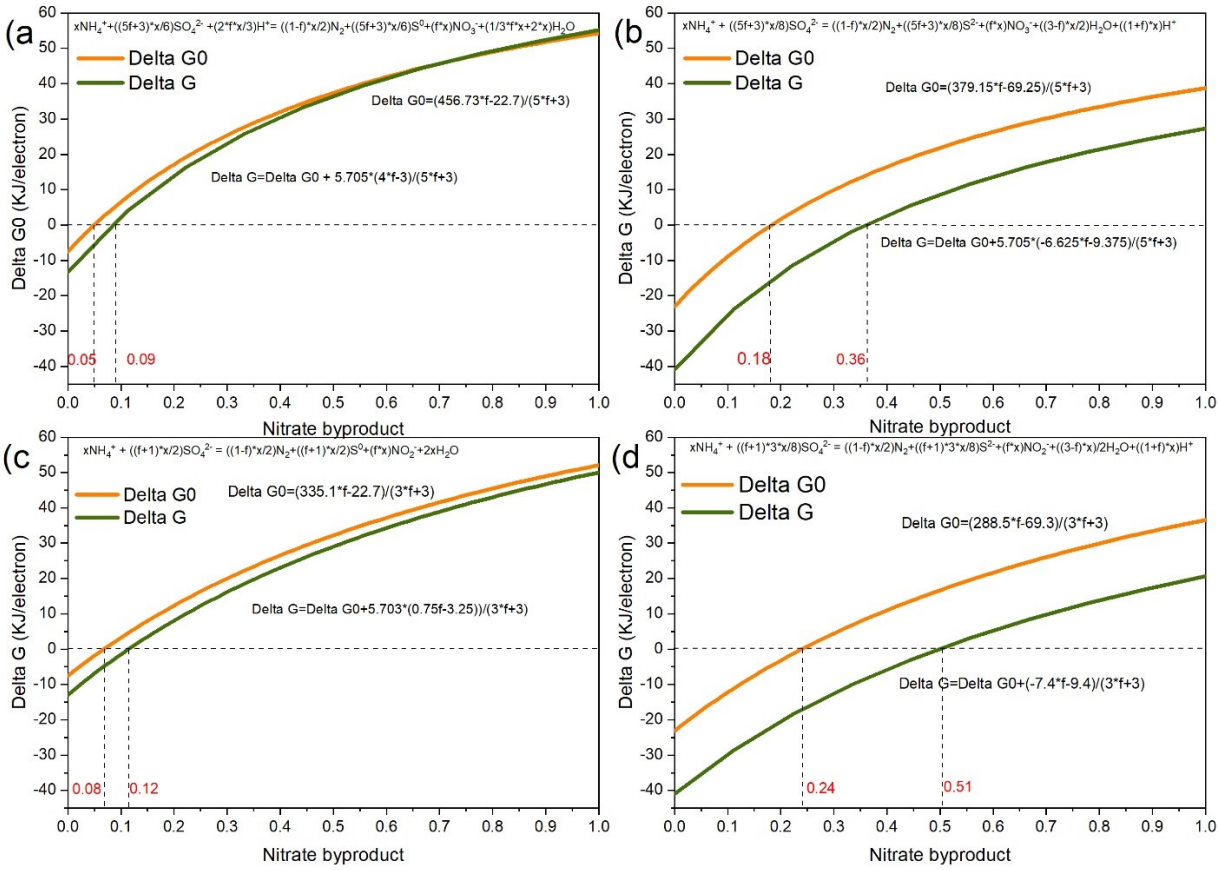

Fig. S2. Gibbs free energy change (KJ/electron) as a function of nitrite/nitrate byproduct proportion: (a) SRAO:N2-NO3--S0; (b) SRAO:N2-NO3--S2-; (c) SRAO:N2-NO2--S0; (d) SRAO:N_2-NO_2^--S^{2-}. The calculations were performed and adjusted to physiological conditions (298.15 K, 1 atm, pH=7).

S6. Methodology to obtain biomass concentration in Table 8

Generally, the reaction rate should be calculated by following equation:

$$Reaction\ rate(mg/g\ VSS/h) = \frac{Substrate\ consumption\ (mg)}{Time(h) * Biomass(g\ VSS/L)}$$

However, the biomass concentration is missing in some of the studies, which needs to be calculated first. After that the reaction rate can be obtained.

For Prachakittikul et al. (2016): the maximum reaction rate was already indicated in the paper as 0.102 g N/g VSS/d and 0.574 g S/g VSS/d at 8 hour. Therefore, the biomass can be reversely calculated as 1.47 g.

For Zhang et al (2023): the VSS concentration was given as 3173 mg/L and the inoculated volume of the batch was 1.5L. Thus, the biomass can be calculated as 3.173*1.5=5.595 g.

For Liu et al. (2008): the VSS concentration was given as 0.0544 g/L, and the inoculated volume of the batch was 100 mL. Thus, the biomass can be calculated as 0.0544*100*10^-3=0.00544 g.

For Lin et al. (2022): the VSS concentration was given as 2.654 g/L, and the inoculated volume of the batch was 250 mL. Thus, the biomass can be calculated as 2.654*250*10^-3=0.6635 g.

For Zhan et al (2023): neither biomass nor reaction rate in the batch test was given. However, the batch test was inoculated by sludge from continuous reactor, where the biomass was 1.78 g VSS/L. The inoculated volume was 200 mL. Thus, biomass in the batch test could be calculated as 1.78*0.2=0.356 g, after which the reaction rate can be calculated.

For Zhu et al. (2022b): neither biomass nor reaction rate of sulfammox phenomenon batch test was given. However, according to another experiment with same incubation in the paper, which was given as "NO_3^--N dropped rapidly from 80 mg/L to 72 mg/L in 30 min with a consumption rate of 17.53 mg N/(g VSS · h)", the biomass amount could be reversely calculated as 0.91 g.

For Wang et al. (2017): although neither VSS nor reaction rate was given, the dataset of this paper was found from Master Thesis Database of Nanjing University. The VSS of the granular sludge used this study was 21.073 g/L, and the inoculated volume of the batch was 0.1L. Thus, the biomass was 21.073*0.1=2.1073 g.

Reference

Fdz-Polanco, F., 2001. New process for simultaneous removal of nitrogen and sulphur under anaerobic conditions. Water Research 35, 1111–1114. https://doi.org/10.1016/S0043-1354(00)00474-7

Kleerebezem, R., Van Loosdrecht, M.C.M., 2010. A Generalized Method for Thermodynamic State Analysis of Environmental Systems. Critical Reviews in Environmental Science and Technology 40, 1–54. https://doi.org/10.1080/10643380802000974

Liu, S., Yang, F., Gong, Z., Meng, F., Chen, H., Xue, Y., Furukawa, K., 2008. Application of anaerobic ammonium-oxidizing consortium to achieve completely autotrophic ammonium and sulfate removal. Bioresource Technology 99, 6817–6825. https://doi.org/10.1016/j.biortech.2008.01.054

Madani, R.M., Liang, J., Cui, L., Zhang, D., Otitoju, T.A., Elsalahi, R.H., Song, X., 2021. Novel simultaneous anaerobic ammonium and sulfate removal process: A review. Environmental Technology & Innovation 23, 101661. https://doi.org/10.1016/j.eti.2021.101661

Qin, Y., Wei, Q., Zhang, Y., Li, H., Jiang, Y., Zheng, J., 2021. Nitrogen removal from ammonium- and sulfate-rich wastewater in an upflow anaerobic sludge bed reactor: performance and microbial community structure. Ecotoxicology 30, 1719–1730. https://doi.org/10.1007/s10646-020-02333-x

Rikmann, E., Zekker, I., Tomingas, M., Tenno, T., Loorits, L., Vabamäe, P., Mandel, A., Raudkivi, M., Daija, L., Kroon, K., Tenno, T., 2016. Sulfate-reducing anammox for sulfate and nitrogen containing wastewaters. Desalination and Water Treatment 57, 3132–3141. https://doi.org/10.1080/19443994.2014.984339

Rikmann, E., Zekker, I., Tomingas, M., Vabamäe, P., Kroon, K., Saluste, A., Tenno, Taavo, Menert, A., Loorits, L., dC Rubin, S.S.C., Tenno, Toomas, 2014. Comparison of sulfate-reducing and conventional Anammox upflow anaerobic sludge blanket reactors. Journal of Bioscience and Bioengineering 118, 426–433. https://doi.org/10.1016/j.jbiosc.2014.03.012

Sabumon, P.C., 2008. Development of a novel process for anoxic ammonia removal with sulphidogenesis. Process Biochemistry 43, 984–991. https://doi.org/10.1016/j.procbio.2008.05.004

Wang, D., Liu, B., Ding, X., Sun, X., Liang, Z., Sheng, S., Du, L., 2017. Performance evaluation and microbial community analysis of the function and fate of ammonia in a sulfate-reducing EGSB reactor. Appl Microbiol Biotechnol 101, 7729–7739. https://doi.org/10.1007/s00253-017-8514-z

Yang, Z., Zhou, S., Sun, Y., 2009. Start-up of simultaneous removal of ammonium and sulfate from an anaerobic ammonium oxidation (anammox) process in an anaerobic up-flow bioreactor. Journal of Hazardous Materials 169, 113–118. https://doi.org/10.1016/j.jhazmat.2009.03.067

Zhang, D., Cui, L., Wang, H., Liang, J., 2019. Study of sulfate-reducing ammonium oxidation process and its microbial community composition. Water Science and Technology 79, 137–144. https://doi.org/10.2166/wst.2019.027

Zhang, L., Zheng, P., He, Y., Jin, R., 2009. Performance of sulfate-dependent anaerobic ammonium oxidation. Sci. China Ser. B-Chem. 52, 86–92. https://doi.org/10.1007/s11426-008-0161-x

Zhao, Q. -l., Li, W., You, S. -j., 2006. Simultaneous removal of ammonium-nitrogen and sulphate from wastewaters with an anaerobic attached-growth bioreactor. Water Science and Technology 54, 27–35. https://doi.org/10.2166/wst.2006.762

Zhu, Y., Yang, S., Wang, W., Meng, L., Guo, J., 2022. Applications of Sponge Iron and Effects of Organic Carbon Source on Sulfate-Reducing Ammonium Oxidation Process. IJERPH 19, 2283. https://doi.org/10.3390/ijerph19042283